The Mössbauer spectra of the three complexes revealed two different quadrupole doublets typical of HS iron(II) instead of only one as seen in case of the ptz complex (see Figure 9). The evaluation of the spectra was even more difficult than for the ptz complex, and for the etz and the iptz complexes satisfactory fits could not be obtained. Not only may texture and an iron(III) impurity similar to that found in the ptz complex be responsible for that but also other unknown impurities may be present.

Unfortunately it was not yet possible to prepare sufficiently pure samples of this class of complexes, but the essential results and statements reported above are not affected by the impurities of the present samples.

Conclusions

The HS $\rightleftharpoons$ LS transition in $[Fe(ptz)_6](BF_4)_2$ induces a first-order phase transition with structural reordering in the vicinity of the iron center. The same phenomenon occurs in a zinc-diluted mixed crystal.

Temperature-dependent spin transition also occurs in the corresponding complexes with other 1-alkyltetrazoles (mtz, etz, iptz) but appears to be more gradual and incomplete, and from the present studies, there is not evidence for a structural phase transition. Unfortunately, it was not possible to prepare sufficiently pure samples of the last three complexes suited for more extensive studies.

Acknowledgment. We wish to thank the Deutsche Forschungsgemeinschaft and the Fonds der Chemischen Industrie for financial support. Dr. P. L. Franke (Rijksuniversiteit Leiden, Leiden, The Netherlands) kindly supplied the samples.

Registry No. $[Fe(mtz)_6](BF_4)_2$, 82285-66-3; $[Fe(etz)_6](BF_4)_2$, 82285-68-5; $[Fe(ptz)_6](BF_4)_2$, 82285-70-9; $[Fe(iptz)_6](BF_4)_2$, 82285-72-1.

Supplementary Material Available: Tables of Mössbauer parameters for the mtz, etz, ptz, and iptz complexes (2 pages). Ordering information is given on any current masthead page.

---

(19) G. Ritter, E. König, W. Irler, and H. A. Goodwin, *Inorg. Chem.*, **17**, 224 (1978).

Contribution from the Departments of Chemistry, University of Washington, Seattle, Washington 98195, and Trinity University, San Antonio, Texas 78284

Laser Raman Spectroscopic Studies of Metal α-Diimine Complexes. 1. Imine Stretching Frequencies and Bonding Implications

WILLIAM H. BATSCHELET*[1] and N. J. ROSE

Received September 22, 1982

Raman spectroscopy was used to accurately and unambiguously determine the imine stretching frequencies for some solid-state transition-metal α-diimine complexes, including those of low-spin Fe(II), and to provide the basis for a critical reevaluation of vibrational assignments for some low-spin Fe(II) complexes. The greatly enhanced sensitivity of the Raman technique compared to infrared spectroscopy led to evidence for the presence of measurable amounts of a low-spin Fe(II) complex at room temperature in a system known to undergo a spin-state transition at lower temperatures. These findings, in turn, allowed an evaluation of the role of the metal's spin state and atomic number in determining the position of the imine stretching frequency of the complex.

Introduction

The α-diimines are neutral, bidentate ligands that are represented by the general structure

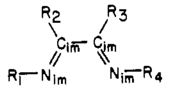

where the R_i may be H, alkyl, or aromatic groups and where the imine linkages may be part of a larger aromatic group as in 2,2'-bipyridine (bpy) or 1,10-phenanthroline (phen). Investigations[2-6] of α-diimine complexes have revealed that the Fe(II) complexes are often unique among first-row transition metals, with this unique nature being attributed to the ability of Fe(II) to donate electron density from its d orbitals into the π^* orbitals on the ligand.[4] One probe for investigating the nature of the metal–ligand interactions has been the dependence of the $M-N_{im}$, $N_{im}-C_{im}$, and $C_{im}-C_{im}$ vibrations on the identity of the metal. Nakamoto performed normal-coordinate analysis for $[Fe(GMI)_3]^{2+}$, $R_1 = R_4 = CH_3$, $R_2 = R_3 = H$, based on the infrared spectrum of the complex and an idealized geometry in which the N atoms were placed at the vertices of an octahedron, and concluded that the $Fe-N_{im}$ stretching force constant was larger than normal while the $N_{im}-C_{im}$ and $C_{im}-C_{im}$ stretching force constants were smaller than those expected for double bonds. Furthermore, he found strong coupling between the in-plane modes of the Fe(GMI) units.[3] In general, however, determining the position of the high-energy stretch ($\sim$1500–1700 cm^{-1}) associated with the five-membered metal α-diimine unit is difficult for many low-spin Fe(II) complexes because of the low infrared intensity of the band.[2,7] Since the imine stretch is a major contributor to this band,[3,8] the inability to definitively observe it has been

---

(1) Trinity University, San Antonio, TX 78284.

(2) Figgins, P. E.; Busch, D. H. *J. Phys. Chem.* **1961**, *65*, 2236.

(3) Nakamoto, K. "Advances in the Chemistry of Coordination Compounds"; Kirschner, S., Ed.; Macmillan: New York, 1961; p 437.

(4) Krumholz, P. *Struct. Bonding (Berlin)* **1971**, *9*, 139.

(5) Batschelet, W. H.; Rose, N. J. "Abstracts of Papers", 172nd National Meeting of the American Chemical Society, San Francisco, CA, Aug 1976; American Chemical Society: Washington, DC, 1976; INOR 201.

(6) Clark, R. J. H.; Turtle, P. C.; Strommen, D. P.; Streusand, B.; Kincaid, J.; Nakamoto, K. *Inorg. Chem.* **1977**, *16*, 84.

(7) Baldwin, D. A.; Pfeiffer, R. M.; Reichgott, D. W.; Rose, N. J. *J. Am. Chem. Soc.* **1973**, *95*, 5152.

(8) (a) Bigotto, A.; Costa, G.; Galasso, V.; DeAlti, G. *Spectrochim. Acta, Part A* **1970**, *26A*, 1939. (b) Bigotto, A.; Galasso, V.; DeAlti, G. *Ibid.* **1971**, *27A*, 1659.

0020-1669/83/1322-2078$01.50/0

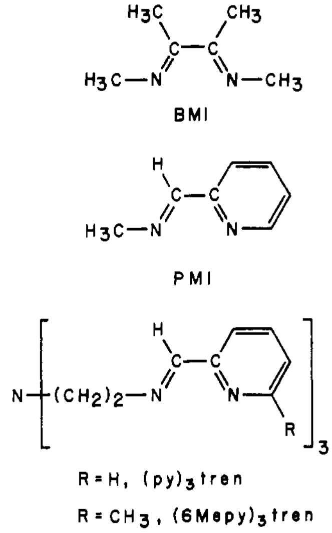

Figure 1. Ligand structures.

a significant handicap in evaluating the effects of Fe(II) on the α-diimine linkage.

By contrast, the Raman spectra of the Fe(II) low-spin species, as well as other various metal α-diimine complexes, clearly show the 1500–1700-cm^{-1} band.[5,9] Nakamoto et al. have demonstrated that the Raman bands associated with the five-membered metal α-diimine unit are especially enhanced for Fe(II) because of the occurrence of resonance Raman scattering arising from the low-energy metal-to-ligand charge-transfer (MLCT) transitions.[6,10]

The purpose of this study was to use Raman spectroscopy in conjunction with previous infrared studies to make unambiguous assignments of the imine stretching frequencies for some α-diimine linkages, especially those coordinated to Fe(II). The detection of these bands in the spectra of the Fe(II) complexes is straightforward due to intensity enhancement from the resonance Raman effect. Because of this sensitivity, our investigation has led to evidence for the presence of low-spin $[Fe(6Mepy)_3tren](PF_6)_2$ at room temperature. This complex is known to exhibit a spin-state crossover but was believed to be exclusively high-spin at room temperature.[11-14] The metal dependency of the metal–α-diimine interaction is also discussed for M(II) complexes with the ligands BMI, PMI, (py)$_3$tren, and (6Mepy)$_3$tren, whose structures are shown in Figure 1.

Ligand Abbreviations. BMI = *N,N'*-(1,2-dimethyl-1,2-ethanediylidene)bis[methanamine], PMI = *N*-(2-pyridylmethylene)methanamine, (py)$_3$tren = tris[4-(2-pyridyl)-3-aza-3-butenyl]amine, and (6Mepy)$_3$tren = tris[4-(6-methyl-2-pyridyl)-3-aza-3-butenyl]amine.

Experimental Section

Table I. Major Raman Peaks of $[ML_3](PF_6)_2$ (Solid)[a]

L = BMI		L = PMI	
M = Fe[b]	M = Ni	M = Fe	M = Co
278 w	373 ms (ν(Ni–N))	279 w	216 s
318 w	444 w, br	368 w	409 w
405 w	739 m	419 m	643 m
478 m (ν(Fe–N))	757 m	432 w	671 w
528 m	802 m, br	515 w	743 m
769 w	945 m	650 w	1022 ms
972 m	989 m	668 m	1112 w
1059 w	1305 m (ν(C–C))	848 w, br	1230 s
1151 w	1405 m	1022 m	1274 w
1336 s (ν(C–C))	1609 s (ν(C=N))	1143 ms	1310 s
1402 m		1164 m	1415 w
1544 s (ν(C=N))		1236 ms	1484 ms
1556 w, sh		1259 m	1574 ms } py
		1303 m	1605 w } py
		1371 w	1634 w, sh
		1411 m	1655 s (ν(C=N))
		1478 s	
		1564 s } py	
		1601 m } py	
		1622 s (ν(C=N))	

[a] Values are given in cm^{-1}; uncertainties in peak locations are ±2 cm^{-1}; relative peak intensities are indicated. [b] Peak locations are close agreement with those observed for aqueous solutions of the iodide salt.[6]

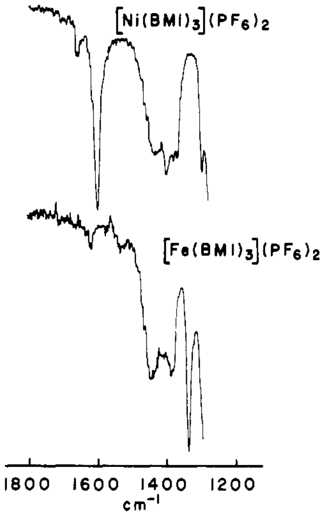

Figure 2. Infrared spectra of $[Ni(BMI)_3](PF_6)_2$ and $[Fe(BMI)_3](PF_6)_2$ as Fluorolube mulls.

Compounds. Starting materials were obtained commercially and were used without further purification. All solvents were reagent grade. $[Fe(BMI)_3](PF_6)_2$, $[Ni(BMI)_3](PF_6)_2$, and $[Fe(6Mepy)_3tren](PF_6)_2$ were prepared according to literature methods.[11,12] The preparations of $[Cu(py)_3tren](PF_6)_2$ and $[Zn(py)_3tren](PF_6)_2$ were derived from the published syntheses[11] with the exception that 4-(2-aminoethyl)-diethylenetriamine (tren) was used directly rather than indirectly by the addition of tren·3HCl and OH$^-$. The samples of $[M(PMI)_3](PF_6)_2$ (M = Fe, Co), $[M(py)_3tren](PF_6)_2$ (M = Mn, Fe, Co, Ni, Cu, and $[Ni(6Mepy)_3tren](PF_6)_2$ had been prepared several years earlier by Wilson.[11] However, their infrared spectra were identical with those in the literature,[2,11] and the samples showed no evidence of decomposition.

Mixed samples of $[Fe/Ni(BMI)_3](PF_6)_2$ were prepared by dissolving the appropriate molar amounts of the pure compounds in acetonitrile and evaporating to dryness. The solids were subsequently powdered and mixed prior to recording their spectra.

Physical Measurements. Raman spectra were recorded with use of a Coherent Radiation Model 52 argon–krypton ion laser, a Spex 1401 double monochromator, an RCA C31034 phototube with dc amplification, and a strip chart recorder. Samples were run as powders

---

(9) Raman intensity arises from a different mechanism than infrared, namely a change in polarizability during a vibration rather than a change in dipole moment. Thus, there is not necessarily a direct correlation between Raman and infrared intensities.

(10) (a) Streusand, B.; Kowal, A. T.; Strommen, D. P.; Nakamoto, K. *J. Inorg. Nucl. Chem.* **1977**, *39*, 1767. (b) Czernuszewicz, R. S.; Nakamoto, K.; Strommen, D. P. *Inorg. Chem.* **1980**, *19*, 793.

(11) Wilson, L. J. Ph.D. Thesis, University of Washington, Seattle, WA, 1971.

(12) Hoselton, M. A.; Wilson, L. J.; Drago, R. S. *J. Am. Chem. Soc.* **1975**, *97*, 1722.

(13) Delker, G. L. Ph.D. Thesis, University of Illinois, Urbana-Champaign, IL, 1976.

(14) Lazarus, M. S.; Hoselton, M. A.; Chou, T. S. *Inorg Chem.* **1977**, *16*, 2549.

Table II. Major Raman Peaks of $[M(6Rpy)_3tren](PF_6)_2$ (Solid)[a]

R = H						R = CH_3	
M = Mn	M = Fe	M = Co	M = Ni	M = Cu	M = Zn	M = Fe	M = Ni
246 m	245 w	272 m	275 m	274 m	242 w	242 w	306 w
439 s	274 m	422 w	361 w	360 w	273 w	272 w	369 w
636 m	351 w	474 w, br	646 m	403 w	322 w	315 w	559 w
740 m	402 m	640 m	667 w	472 w	351 w	400 w	595 w
870 m	514 w	669 w	746 m	645 m	459 w, br	455 w	744 w
1011 s	651 m	745 w	779 w	664 m	509 w	488 w, br	773 w
1061 m	662 m	875 w	816 w	740 m	575 w, br	528 w	909 w
1113 w	1023 m	912 w	879 w	776 w	639 m	557 w	1011 ms
1222 s	1075 w, br	957 w	925 w	816 w	668 w	657 w	1078 m
1344 w	1116 w	1014 ms	960 w	859 w	746 m	768 w	1227 ms
1384 w	1163 m	1063 w	997 w	874 w	873 w, br	864 w	1288 ms
1472 w	1216 m	1074 m	1025 ms	924 w	961 w	909 w	1318 m
1481 m	1234 m	1114 w	1060 w	960 w	1003 m	1008 m	1335 m
1576 ms	1263 w	1165 w	1082 w	975 w	1014 m	1026 w	1484 m
1602 m	1304 m	1228 s	1114 m	997 m	1058 m, br	1076 w	1563 w
1668 s	1350 w	1268 w	1163 w	1023 ms	1083 w	1116 w	1574 ms
	1376 w	1347 w	1181 w	1058 m	1111 m	1178 w	1661 s
	1475 s	1381 w	1226 ms	1078 m	1165 w	1223 m	
	1561 s	1482 ms	1278 w	1111 m	1223 s	1240 w	
	1594 m	1574 ms	1311 m	1166 w	1287 w	1265 w	
	1616 s	1603 m	1336 m	1227 s	1312 w	1284 m	
		1662 s	1386 w	1274 w	1344 m	1409 m, br	
			1455 w	1309 m	1376 w	1471 m	
			1574 ms	1341 m	1383 w	1561 ms	
			1603 m	1382 w	1450 w	1568 m	
			1653 s	1456 m	1468 w	1600 m	
				1482 m	1483 m	1629 ms[c]	
				1561 m[b]	1577 ms	1652 s[d]	
				1574 ms[b]	1601 m		
				1596 w[b]	1668 s		
				1604 m[b]			
				1613 w[b]			
				1655 s			

[a] Values are given in cm^{-1}; uncertainties in peak locations are ±2 cm^{-1}; relative peak intensities are indicated. [b] The multiplicity in this region is due to splitting of the py I and py II bands because of a Jahn–Teller distortion in the Cu(II) complex (see ref 11). [c] Low-spin imine stretch. [d] High-spin imine stretch.

in capillary tubes, and no correction was made for phototube response. Infrared spectra were recorded with a Beckman IR 10 spectrophotometer.

Results and Discussion

The solid-state Raman spectra for the $[ML_3](PF_6)_2$ and $[M(6Rpy)_3tren](PF_6)_2$ complexes are summarized in Tables I and II.

BMI. Figure 2 gives a portion of the infrared spectra of $[Ni(BMI)_3](PF_6)_2$ and $[Fe(BMI)_3](PF_6)_2$. The strong absorbance at 1608 cm^{-1} for the Ni(II) complex has been assigned as the imine stretching mode, and a value of 1540 cm^{-1} has been estimated for the Fe(II) complex[4] although any such assignment in the 1500–1700-cm^{-1} region is tentative at best. The Raman spectra of these complexes in the same region are given in Figure 3. Again, the $[Ni(BMI)_3](PF_6)_2$ has an intense peak at 1609 cm^{-1} arising from the imine stretch. Unlike the infrared, the Raman spectrum of $[Fe(BMI)_3](PF_6)_2$ in this region is similar to that of the Ni(II) complex, and the intense peak at 1544 cm^{-1} is assigned as the imine stretch. This differs from the previous Raman assignment of the imine stretch to the 1400-cm^{-1} band.[6] As seen in Figure 3 and Table I, the band in the 1400-cm^{-1} region varies only slightly in position between the Fe(II) and Ni(II) complexes, while the band in the 1500–1600-cm^{-1} region is much more sensitive to metal identity. Thus, the higher energy bands are assigned as imine stretches, while the band near 1400 cm^{-1} in both spectra is attributed to the asymmetric deformations of the methyl groups of the BMI.[15]

Table III. Fe:Ni Raman Peak Height Ratio as a Function of Exciting Frequency for $[(Fe/Ni)(BMI)_3](PF_6)_2$ (Mixed Solid)[a]

Fe/Ni peak location, cm^{-1}	exciting freq, nm			
	647.1	568.2	514.5	488.0
1556/1609	0.9	9.2	5.0	1.9
1336/1305	3.5	35.1	11.3	9.4

[a] Fe:Ni = 1:80.

As shown in Table III by the relative peak heights of a mixed Fe/Ni sample, the Raman intensity of $[Fe(BMI)_3]^{2+}$ is roughly 2 orders of magnitude greater than that of $[Ni(BMI)_3]^{2+}$ at an exciting frequency of 647.1 nm. The Raman intensity of the Fe(II) complex is further enhanced by resonance Raman scattering, which occurs when the exciting frequency falls within the intense MLCT bands of the complex.[6,10] The vibrational modes that show enhanced Raman intensity are those vibronically active in the electronic transition, i.e., those associated with the Fe(II)–diimine chromophore.[6] This was shown by Nakamoto et al. with the Raman excitation profiles of $[Fe(BMI)_3]^{2+}$ [6] and is further demonstrated by the data in Table III. As the exciting frequency approaches the maximum in the charge-transfer absorption at 568 nm,[16] the relative Raman intensities of the Fe(II) complex are greatly increased.

For $[Fe(BMI)_3]^{2+}$, the peaks at 1336 and 478 cm^{-1} (Table I) are tentatively assigned as predominantly C_{im}–C_{im} and Fe–N stretches, respectively. Both of these bands have strong intensity dependence upon the exciting frequency[6] and a strong dependence upon the metal ion, shifting to 1305 and 373 cm^{-1}

---

(15) Colthrup, N. B.; Daly, L. H.; Wiberly, S. E. "Introduction to Infrared and Raman Spectroscopy", 2nd ed.; Academic Press: New York, 1975.

(16) Krumholz, P. *J. Am. Chem. Soc.* **1953**, *75*, 2163.

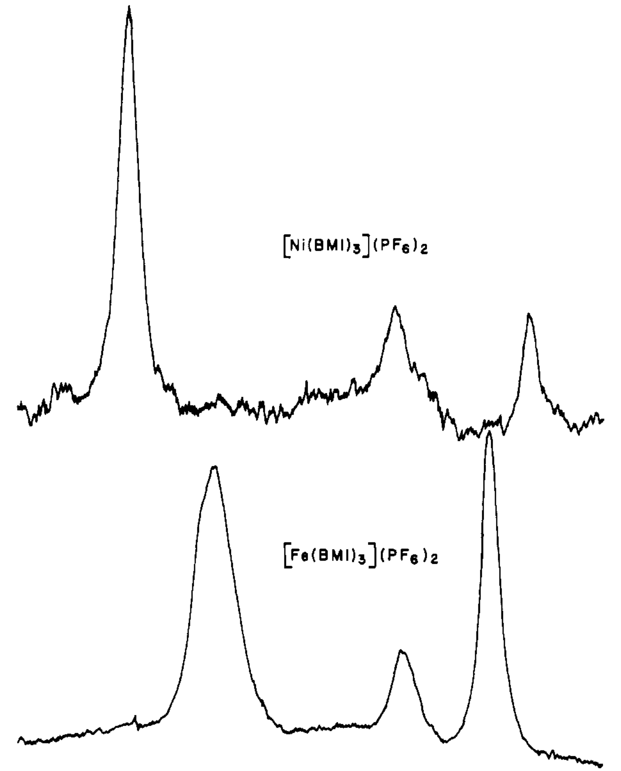

Figure 3. Raman spectra of $[Ni(BMI)_3](PF_6)_2$ and $[Fe(BMI)_3](PF_6)_2$ in the solid state.

in the $[Ni(BMI)]_3{}^{2+}$ complex. The assignment for the 1300-cm^{-1} band is supported by the vibrational assignments for 1,2,5-oxadiazole and related compounds (**1**), which also have a band in that region assigned as a ring stretch.[17] For the M–N stretch, the difference of 105 cm^{-1} between the Fe(II) and Ni(II) complexes is essentially the same as that observed for the corresponding $[M(bpy)_3]^{2+}$ or $[M(phen)_3]^{2+}$ complexes.[18]

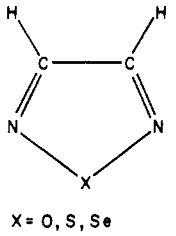

1

PMI. The Raman bands for $[Fe(PMI)_3](PF_6)_2$ and $[Co(PMI)_3](PF_6)_2$ are summarized in Table I. In keeping with previous infrared assignments for $[Co(PMI)_3]^{2+}$,[2] the strong band at 1655 cm^{-1} is assigned as the imine stretch while the bands at 1605 and 1574 cm^{-1} are attributed to vibrations of the pyridine groups and assigned as py I and py II, respectively. For $[Fe(PMI)_3]^{2+}$, the bands at 1601 and 1564 cm^{-1} are assigned as py I and py II on the basis of intensities similar to those of $[Co(PMI)_3]^{2+}$ and the fact that the pyridine bands have been shown to be relatively insensitive to substituent effects[15] or to metal identity.[19] The imine stretch is assigned to the strong band at 1622 cm^{-1}, unlike the previous assignment of 1558 cm^{-1}, which was based on infrared intensity arguments.[2]

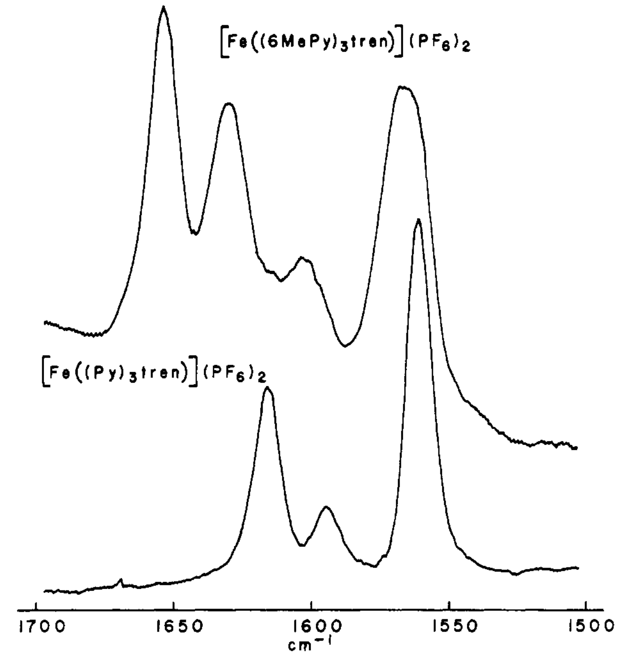

Figure 4. Room-temperature Raman spectra of $[Fe(py)_3tren](PF_6)_2$ and $[Fe(6Mepy)_3tren](PF_6)_2$.

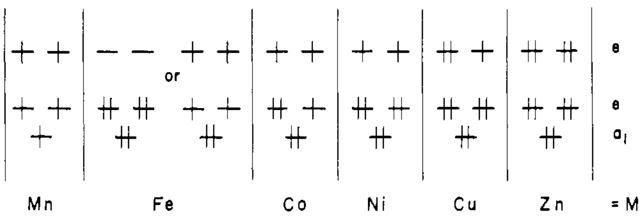

Figure 5. Crystal field diagrams for an M(II) ion in D_3 symmetry.

(6Rpy)$_3$tren. The Raman spectra for $[M(py)_3tren]^{2+}$ (M = Mn(II), Fe(II), Co(II), Ni(II), Cu(II), Zn(II)) and $[M(6Mepy)_3tren]^{2+}$ (M = Fe(II), Ni(II)) are summarized in Table II. The value for the imine stretching frequency of $[Fe(py)_3tren]^{2+}$ had not been previously assigned by infrared spectroscopy. However, as with $[Fe(PMI)_3]^{2+}$, the Raman assignment of 1616 cm^{-1} is straightforward. For the remainder of the $[M(py)_3tren]^{2+}$ series, the assignments of the imine stretching frequencies to the peaks in the 1650–1670-cm^{-1} region (Table II) agree well with those determined from infrared spectra.[11]

The room-temperature Raman spectrum of $[Fe(6Mepy)_3tren]^{2+}$ is unique in that it has two distinct peaks in the 1615–1670-cm^{-1} region that contained the imine stretches of the $[M(py)_3tren]^{2+}$ series (Table II, Figure 4). The two peaks are properties of the complex itself and are not due to solid-state effects since the Raman spectra of $[Fe(6Mepy)_3tren]^{2+}$ in acetonitrile or acetone solutions also contain these peaks.[20] This complex is known to undergo a spin-state transition, going from high to low spin as the temperature is decreased; however, it was believed to be exclusively high spin at room temperature.[11-14] The peak at 1652 cm^{-1}, which is also present in the infrared spectrum,[11] is assigned as the imine stretching frequency of high-spin $[Fe(6Mepy)_3tren]^{2+}$ while that at 1629 cm^{-1} is assigned to the low-spin complex. These assignments, which have been con-

---

[17] Dollish, F. R.; Fateley, W. G.; Bentley, F. F. "Characteristic Raman Frequencies of Organic Compounds"; Wiley: New York, 1974.

[18] Hutchinson, B.; Takemoto, J.; Nakamoto, K. *J. Am. Chem. Soc.* **1970**, *92*, 3335.

[19] Gill, N. S.; Nuttall, R. H.; Scaife, D. E.; Sharp, D. W. A. *J. Inorg. Nucl. Chem.* **1961**, *18*, 79.

[20] Batschelet, W. H.; Rose, N. J. *Inorg. Chem.*, following paper in this issue.

Table IV. Values of $\nu(C{=}N)$ for $[ML_3]^{2+}$ Complexes[a]

L	Fe	Co	Ni	Cu
BMI	1544	1608[b]	1609	
PMI	1622	1655	1654[b]	1655[b]

[a] Values given in cm^{-1}. [b] See ref 2; values are based on infrared spectra.

firmed by low-temperature infrared spectroscopy[13] and by variable-temperature Raman spectroscopy,[20] provide the first evidence for the existence of the low-spin species at room temperature.

Bonding Implications. The factors that govern the metal–ligand interactions are the amount of orbital overlap between metal- and ligand-centered orbitals, the similarity in the energies of these orbitals, and the number of electrons involved, with the type of interactions between symmetry determined. The idealized symmetry for a tris(α-diimine) complex is D_3 or C_3, depending on the ligand. The crystal field diagrams for the Mn(II)–Zn(II) ions in D_3 symmetry are given in Figure 5. The upper two orbitals (e) are primarily σ^* with respect to the metal–ligand bond while the lower three orbitals (e and a_1) have essentially π symmetry. The ordering of the lower three orbitals may possibly be reversed, depending on the nature of the metal–ligand interactions. The a_1 orbital of D_3 symmetry correlates with an a orbital in C_3 symmetry, whereas the labelings of the e orbitals are the same in both symmetries.

Of particular interest in α-diimine systems are interactions between the metal and the lowest unoccupied ligand π^* orbital. Calculations indicate that this orbital is N_{im}–C_{im} antibonding and C_{im}–C_{im} bonding for a variety of α-diimines.[21-23] Delocalization of electron density from the metal into this orbital would weaken the N_{im}–C_{im} bond while strengthening the M–N_{im} and C_{im}–C_{im} bonds. These effects can be seen in the changes in bpy bond lengths in the complex Mo(O-*i*-Pr)$_2$(bpy)$_2$ where the authors estimate that a net negative charge of approximately 0.5 e is transferred into the lowest π^* orbital of each bpy.[24] A similar trend in ligand interatomic distances has been noted for $[Fe(py)_3tren]^{2+}$ [25a] and in the structure of a tetraazadiene complex.[26] Also consistent with increased π delocalization in $[Fe(py)_3tren]^{2+}$ is the fact that its imine stretching frequency is the lowest of the series (Table II). The changes in the imine stretches are readily observed while the structural differences are only marginally significant.[25] Thus, imine stretching frequencies prove to be a sensitive and readily identifiable probe of the changes in metal–α-diimine interactions.

Table IV summarizes the imine stretching frequencies for some $[ML_3]^{2+}$ complexes. For both the BMI and PMI complexes, the values are significantly lower with Fe(II). Fe(II) is the only low-spin ion among the complexes in this study and has no electrons in the e(σ^*) orbitals (Figure 5). On this basis it would be expected to have the strongest M–N_{im} bond, shortest M–N_{im} distance, and greatest metal–ligand orbital overlap. Because there is no electron density in the σ^* orbitals, low-spin Fe(II) should be the best σ acceptor. This would lead to an increased N_{im}–C_{im} σ-bond strength since calculations indicate that the nitrogen lone pair is antibonding with respect to the imine σ bond.[27] Additionally, Fe(II) would be the best π donor among the M(II) ions studied. It has the maximum number of electrons in orbitals capable of π donation (Figure 5), greatest 3d–2p π overlap, and a relatively high Lewis basicity.[28] Although the actual differences in σ- and π-bond strengths are not known, delocalization of electron density from the iron into the π^* orbital leads to an overall decrease in N_{im}–C_{im} bond strength greater than any expected increase in the σ system as evidenced by the lower imine stretches of the iron complexes. The facts that the C_{im}–C_{im} and M–N_{im} stretching frequencies are greater for $[Fe(BMI)_3]^{2+}$ are also consistent with increased π donation in the Fe(II) complex (vide supra), although σ effects must also play a significant role in the difference between the M–N_{im} stretches for the two complexes.

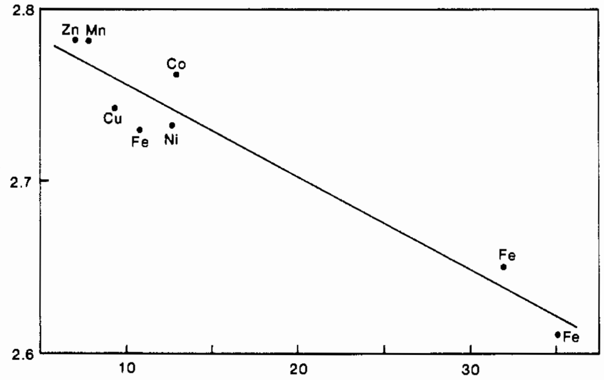

Figure 6. Dependency of imine stretching frequency squared on M–N π overlap and number of d π electrons for the $[M(6Rpy)_3tren](PF_6)_2$ series.

The $[M(6Rpy)_3tren]^{2+}$ complexes provide a more extensive series for evaluating metal–α-diimine interactions. On the assumption that (wave number)^2 is proportional to the vibrational force constant of the imine bond and with use of the quantity nS^2 as a measure of the metal–ligand π interaction (n = number of d π electrons, S = M–N_{im} 3d–2p π overlap[29]), Figure 6 illustrates that a strong correlation exists between (wave number)^2 and nS^2. Within the $[M(py)_3tren]^{2+}$ series, the Fe(II) complex has the maximum number of electrons in orbitals capable of π donation (Figure 5), the highest M–N_{im} π overlap, and the lowest imine stretch. The Mn(II) and Zn(II) complexes have the highest imine stretches (Table II) consistent with the smallest number of electrons present or smallest orbital overlap, respectively. The variations between the experimental values and the best fit line are probably due to changes in the σ-bond strength and to individual differences in metal ion orbital energies, both of which were treated as constant.

The $[Fe(py)_3tren]^{2+}$ and $[Fe(6Mepy)_3tren]^{2+}$ complexes provide a basis for comparison in which there is no change in metal identity. Replacement of H by CH_3 leads to increased steric interaction between the arms of the ligand[11] and an increase in the Fe–N_{im} bond distances.[13,25] This leads to a decrease in the Fe–N_{im} overlap, and the imine stretch increases by 13 cm^{-1} on going from $[Fe(py)_3tren]^{2+}$ to low-spin [Fe-

---

(21) Hanazaki, I.; Nagakura, S. *Inorg. Chem.* **1969**, *8*, 648.

(22) Norman, J. G., Jr.; Chen, L. M. L.; Perkins, C. M.; Rose, N. J. *Inorg. Chem.* **1981**, *20*, 1403.

(23) Benedix, R.; Reinhold, J.; Hennig, H. *Inorg. Chim. Acta* **1980**, *40*, 47.

(24) Chisholm, M. H.; Huffman, J. C.; Rothwell, I. P.; Bradley, P. G.; Kress, N.; Woodruff, W. H. *J. Am. Chem. Soc.* **1981**, *103*, 4945.

(25) (a) Mealli, C.; Lingafelter, E. C. *J. Chem. Soc., Chem. Commun.* **1970**, 885. (b) Kirchner, R. M. Ph.D. Thesis, University of Washington, Seattle, WA, 1971. (c) Torre, L. P. Ph.D. Thesis, University of Washington, Seattle, WA, 1971. (d) Lingafelter, E. C., private communication.

(26) Gross, M. E.; Trogler, W. C.; Ibers, J. A. *J. Am. Chem. Soc.* **1981**, *103*, 192.

(27) Batschelet, W. H. Ph.D. Thesis, University of Washington, Seattle, WA, 1977.

(28) Mn(II) has a smaller effective nuclear charge than Fe(II), and low-spin Mn(II) should have a high M–N_{im} 3d–2p overlap. However, Mn(II) has one less electron in the 3dπ orbitals and would not be as effective a π donor as low-spin Fe(II).

(29) Overlaps were calculated by using distances found in the single-crystal X-ray structures[13,25] and neutral-atom wave functions (Roetti, C.; Clementi, E. *J. Chem. Phys.* **1974**, *60*, 3342).

(6Mepy)$_3$tren]$^{2+}$ (Table II, Figure 6). Upon conversion to high-spin [Fe(6Mepy)$_3$tren]$^{2+}$ there is a decrease in the number of electrons in π orbitals (Figure 5) and a further increase in the Fe–N$_{im}$ bond distance.[13] Both of these effects lead to decreased metal–ligand interaction, and the imine stretching frequency increases another 23 cm^{-1} (Figure 6).

Conclusions

Raman spectroscopy is a sensitive technique for accurately determining the imine stretching frequency in low-spin Fe(II) α-diimine complexes. This is due, at least in part, to the low-energy MLCT transitions of these compounds that lead to resonance Raman enhancement as the exciting frequency approaches that of the MLCT.[6] This special sensitivity is illustrated by [Fe(PMI)$_3$]$^{2+}$, for which previous assignments[4] of the imine stretch based on infrared spectra were incorrect. It is further demonstrated by the Raman spectrum of [Fe(6Mepy)$_3$tren]$^{2+}$ for which both the high- and low-spin forms are observed at room temperature. This represents the first time that the low-spin species has been observed at room temperature. It seems likely that this technique should be applicable to other metal–imine systems that contain metals such as Cu(I), Cr(0), and Ru(II) in lower oxidation states and in which the imine stretches appear to have unusual behavior on the basis of infrared spectroscopy.[30–32]

Although the actual amounts of electron delocalization from metal to α-diimine π^* orbitals are not known, the trends in imine stretching frequency allow a qualitative evaluation of the importance of π delocalization and some of the factors affecting it. For all of the complexes in this study, it is most extensive with low-spin Fe(II), where there are the maximum number of electrons available for donation and the highest metal–ligand overlaps. Even then, the imine stretches are still in the region expected for double bonds, indicating that the overall changes in N$_{im}$–C$_{im}$ bond strength are relatively small.

Acknowledgment. Support provided through Grant CHE74-19328A02 from the National Science Foundation is gratefully acknowledged.

Registry No. [Fe(BMI)$_3$](PF$_6$)$_2$, 85828-60-0; [Ni(BMI)$_3$](PF$_6$)$_2$, 85828-62-2; [Fe(PMI)$_3$](PF$_6$)$_2$, 36487-65-7; [Co(PMI)$_3$](PF$_6$)$_2$, 36465-55-1; [Mn(py)$_3$tren](PF$_6$)$_2$, 85828-68-8; [Fe(py)$_3$tren](PF$_6$)$_2$, 55222-32-7; [Co(py)$_3$tren](PF$_6$)$_2$, 63526-13-6; [Ni(py)$_3$tren](PF$_6$)$_2$, 56348-41-5; [Cu(py)$_3$tren](PF$_6$)$_2$, 85828-64-4; [Zn(py)$_3$tren](PF$_6$)$_2$, 85828-66-6; [Fe(6Mepy)$_3$tren](PF$_6$)$_2$, 55190-36-8; [Ni(6Mepy)$_3$tren](PF$_6$)$_2$, 56348-47-1.

---

(30) Gagné, R. R.; Ingle, D. M.; Lisensky, G. C. *Inorg. Chem.* **1981**, *20*, 1991.
(31) King, R. B.; Douglas, W. M. *J. Am. Chem. Soc.* **1973**, *95*, 7528.
(32) Lane, B. C.; Lester, J. E.; Basolo, F. *J. Chem. Soc. D* **1971**, 1618.

Contribution from the Departments of Chemistry, University of Washington,
Seattle, Washington 98195, and Trinity University, San Antonio, Texas 78284

Laser Raman Spectroscopic Studies of Metal α-Diimine Complexes. 2. Studies of a Spin-Equilibrium System

WILLIAM H. BATSCHELET*[1] and N. J. ROSE

Received September 22, 1982

Raman spectroscopy was used to differentiate between high- and low-spin Fe(II) in [Fe(6Mepy)$_3$tren]$^{2+}$ spin-crossover systems on the basis of differences in the imine stretching region (1600–1700 cm^{-1}). The spin equilibria of the complex in solution and in the solid state as PF$_6^-$, BF$_4^-$, and BPh$_4^-$ salts were studied. The spin crossovers are adequately described by using a Boltzmann distribution between two states with an incomplete transition occurring for the BPh$_4^-$ salt. Factors affecting the equilibria are discussed, and an explanation of the discrepancies between the Raman data and other physical measurements is given in terms of resonance-Raman enhancement of the low-spin Fe(II) imine band and the nucleation and growth mechanism of phase transitions in solids.

Introduction

Octahedral and pseudooctahedral transition-metal complexes having d^4–d^7 configurations exist in either high-spin or low-spin electronic ground states, depending on the nature of the ligating atoms. For a relatively small number of complexes, the properties of the ligands are such that the energy differences between the high- and low-spin states are on the order of kT. The result is a spin crossover or spin equilibrium, and a number of spin-crossover systems and their properties have been reviewed.[2–8]

For compounds having spin crossovers, the fraction of molecules in the high-spin state decreases with decreasing temperature, often with a dramatic transition from high to low spin occurring over a few degrees. In addition, incomplete transitions to fully low-spin (residual paramagnetism) or fully high-spin states have been observed in which the ratio of high- to low-spin molecules reaches a plateau.[2,3] Various models have been proposed to explain these phenomena,[2,3] and recently Hendrickson and co-workers[9–11] used the nucleation and growth mechanism of phase transitions[12,13] in solids to explain

---

(1) Trinity University.
(2) Gütlich, P. *Struct. Bonding (Berlin)* **1981**, *44*, 83.
(3) Goodwin, H. A. *Coord. Chem. Rev.* **1976**, *18*, 293.
(4) Martin, R. L.; White, A. H. *Transition Met. Chem. (N.Y.)* **1968**, *4*, 113.
(5) Barefield, E. K.; Busch, D. H.; Nelson, S. M. *Q. Rev., Chem. Soc.* **1968**, *22*, 457.
(6) König, E. *Coord. Chem. Rev.* **1968**, *3*, 471.
(7) Sacconi, L. *Pure Appl. Chem.* **1971**, *27*, 161.
(8) König, E. *Ber. Bunsenges. Phys. Chem.* **1972**, *76*, 975.
(9) Haddad, M. S.; Federer, W. D.; Lynch, M. W.; Hendrickson, D. N. *J. Am. Chem. Soc.* **1980**, *102*, 1470.
(10) Haddad, M. S.; Lynch, M. W.; Federer, W. D.; Hendrickson, D. N. *Inorg. Chem.* **1981**, *20*, 123.
(11) Haddad, M. S.; Federer, W. D.; Lynch, M. W.; Hendrickson, D. N. *Inorg. Chem.* **1981**, *20*, 131.
(12) Rao, C. N. R.; Rao, K. J. "Phase Transitions in Solids"; McGraw-Hill: New York, 1978.

0020-1669/83/1322-2083$01.50/0